Journal of Physical Science, Vol. 31(2), 15–31, 2020

Preparation and Characterisation of Blend Cellulose Acetate Membrane for CO_2/N_2 Separation

Reinie Pui Wong Xiao Jin,[1] Zeinab Abbas Jawad,[1*] Peng Chee Tan,[2] Bridgid Lai Fui Chin,[1] Thiam Leng Chew[3,4] and Agus Saptoro[1]

[1]Department of Chemical Engineering, Faculty of Engineering and Science, Curtin University Malaysia, CDT 250, 98009 Miri, Sarawak, Malaysia
[2]School of Energy and Chemical Engineering, Xiamen University Malaysia, Jalan Sunsuria, Bandar Sunsuria, 43900 Sepang, Selangor, Malaysia
[3]Department of Chemical Engineering, Faculty of Engineering, Universiti Teknologi PETRONAS, 32610 Seri Iskandar, Perak, Malaysia
[4]CO_2 Research Centre (CO2RES), Institute of Contaminant Management, Universiti Teknologi PETRONAS, 32610 Seri Iskandar, Perak, Malaysia

[*]Corresponding author: zeinab.aj@curtin.edu.my

Published online: 25 August 2020

To cite this article: Jin, R. P. W. X. et al. (2020). Preparation and characterisation of blend cellulose acetate membrane for CO_2/N_2 separation. *J. Phys. Sci.*, 31(2), 15–31. https://doi.org/10.21315/jps2020.31.2.2

To link to this article: https://doi.org/10.21315/jps2020.31.2.2

ABSTRACT: *Among the carbon dioxide (CO_2) separation methods, the membrane separation technology has been mostly applied to reduce the CO_2 emission. Since most CO_2 are emitted from power generation plants, the CO_2/nitrogen (N_2) separation was selected. In this project, the blend cellulose acetate (CA) membranes were prepared by mixing CA with 39% acetyl concentration (CA-39) and 56% acetyl content (CA-56) through the wet-phase inversion method. The CO_2/N_2 separation performance was determined by evaluating the permeation of gases and the CO_2/N_2 selectivity by modifying the polymer concentration. The characterisation of the membrane was carried out by using the scanning electron spectrometry (SEM) and attenuated total reflectance Fourier transform infrared spectrometry analysis (ATR-FTIR). The optimal membrane obtained was M3 with polymer concentration of 4:6 (CA-39:CA-56) that had defect-free membrane surface with smooth dense skin layer. The functional groups present enhanced the gas permeance rate. With regards to the gas permeation test, M3 presented the best CO_2/N_2 separation performance with CO_2 permeance of 99.26 ± 3.08 GPU, N_2 permeance of 87.12 ± 0.81 GPU and CO_2/N_2 selectivity of 1.139 ± 0.037. It is expected that the results obtained from this work can be applied to industries, such as the gas separation field or power generation plant, in order to reduce CO_2 emission.*

Keywords: Membrane technology, gas separation, cellulose acetate, polymer concentration

1. INTRODUCTION

Membrane technology is one of the gas separation methods that can effectively reduce the carbon dioxide (CO_2) emission.[1,2] It has advantages such as being high energy efficiency, cheap, environmentally-friendly and simplicity.[3,4] Since CO_2 are mostly emitted from power generation plant, the CO_2/nitrogen (N_2) separation should be more effective to reduce the CO_2 emission rate.[5,6] Based on Feron et al., the cellulose acetate (CA) holds the greatest promise in membrane material selection because it has the highest CO_2/N_2 selectivity compared with other polymeric materials.[7] Moreover, CA has many advantages such as being low cost and environmentally friendly, which causes CA to be more preferable compared to the other polymeric materials.[8,9] There are two types of CA polymers used in this study, which are CA with acetyl content of 56% (CA-56) and CA with acetyl content of 39% (CA-39).

To improve the gas separation performance, the most important parameter is the polymer concentration. Aroon et al. reported that the polymer concentration increased with the gas selectivity but formed a thicker skin layer and thus, reduced the gas permeability.[10] According to Hacarlioglu et al., a higher polymer concentration was preferable; however, it cannot exceed certain limits due to the high permeability and low selectivity of polymeric membranes.[11] Many works summarised that the increment in polymer concentration decreased the membrane permeability and increased the gas selectivity.[10–12] Therefore, the main aim of this research is to develop a thin, defect-free blend CA-39/CA-56 membrane, which can enhance the permeance of CO_2 and increase the selectivity of CO_2/N_2. Up to date, the study on polymer concentration for blend CA membranes with various acetyl concentrations (CA-39 and CA-56) has not been investigated.

2. EXPERIMENTAL

2.1 Materials

The CA (acetyl content: 54.5%–56.0%) was obtained from Sinopharm Chemical Reagent Co. Ltd., China while the CA (acetyl content: 39.8%) and acetic acid (CH_3COOH), ACS reagent $\geq$ 99.7%, were acquired from Sigma-Aldrich, Malaysia. Ethanol and n-Hexane were purchased from Merck, Malaysia.

2.2 CA Membrane Fabrication

A mixture of 10 wt% of CA, 63 wt% of acetic acid and 27 wt% of deionised water was stirred and heated to 55°C by a heating plate for 3 h until the CA polymer

completely dissolved in the solution. Thereafter, the solution was cooled until it reached ambient temperature of 27°C. After that, the cooled solution at ambient temperature was stirred for another 12 h and then sent for ultrasonic degassing (ELMASONIC S60H, Germany) to prevent the formation of bubbles. The casting thickness of the sample membrane was adjusted by using the Automatic Film Applicator (Malaysia) at ambient room temperature. Then, the sample membrane was submerged into a deionised water bath for 5 min. Next, it was moved to another water bath and immersed for one day in order to eliminate any excess solvent remaining in the sample membrane. To dry the membrane, the sample membrane was submerged into fresh ethanol for 4 h and then submerged into n-hexane solution for another 1 h. The final CA membrane was located between two glass plates and dried for one day. Finally, the final CA was stored and ready for further testing.[13] The percentage of polymer-solvent mixture was determined from previous works.[14,15] The casting thickness of the membrane was fixed at 250 μm and the composition for the membranes were illustrated in Table 1.

Table 1: Compositions of membrane fabrication.

Sample	Polymer-solvent mixture			CA polymer content	
	CA (wt%)	Acetic acid (wt%)	Water (wt%)	CA-39 (wt%)	CA-56 (wt%)
M1	10	63	27	1	9
M2	10	63	27	2	8
M3	10	63	27	4	6
M4	10	63	27	5	5

2.3 Gas Permeation Test

To examine the permeation of gas, a gas permeation test was conducted based on previous published work.[13] The volume displacement method was used to determine the flowrate of both output streams individually by using soap bubble flow meters. The permeability of membrane (P/l) was determined by Equation 1 and indicated in GPU.[15]

$$\frac{P}{l} = \frac{Q}{A\Delta p} \tag{1}$$

where:
l = membrane thickness (cm)
A = effective membrane area (cm^2)
Q = Measured volumetric flowrate in standard temperature and pressure ($cm^3\ s^{-1}$)
Δp = Pressure difference through the membrane (cmHg)

$$1\ \text{GPU} = 1 \times 10^{-6}\ \frac{cm^3(\text{STP})}{cm^2\ s\ cmHg}$$

Furthermore, the selectivity of gases can be determined by studying the gas separation performance. The formula used to calculate the CO_2/N_2 selectivity was expressed in Equation 2.[16]

$$\alpha_{CO_2/N_2} = \frac{P_{CO_2}}{P_{N_2}} \tag{2}$$

where α_{CO_2/N_2} is the ideal selectivity of CO_2/N_2.

2.4 Membrane Characterisation

2.4.1 SEM

The surface morphology of the synthesised membranes was investigated through a scanning electron microscopy (SEM) (Hitachi TM3000). The membrane samples were broken into small pieces and frozen at –80°C for one day to obtain an ordinarily steady and neat cut. The samples were then sputter-coated with thin gold film to avoid sample charging, which caused the contrasting structure. Next, the samples were placed inside the SEM to collect the cross-sectional structure of the membranes. A minimum of five membrane samples were used in this characterisation to examine the consistency of the samples.[17,18]

2.4.2 ATR-FTIR Spectroscopy Analysis

The attenuated total reflectance-Fourier transform infrared (ATR-FTIR) was used to record the spectra, amend their baselines, systematise the spectra, and detect the peaks value through theNicolet IS10 (USA) spectrometer with wave numbers ranging from 450 cm^{-1} to 4000 cm^{-1} at 4 cm^{-1} resolution.[19] Spectra specimens were collected with 32 scans setting. The spectra wavenumbers of membrane specimens were recorded at ambient room temperature and repeated few times for every specimen.[14,20]

3. RESULTS AND DISCUSSION

3.1 Effects of Polymer Concentration of CA with Different Acetyl Contents

In order to understand the interaction effects of the gas separation membranes, the membrane properties were determined and membrane characterisation was carried out for developing a new enhanced membrane-based gas separation. In this study, the CA membranes were blended at different polymer ratios of CA-39 and CA-56

at 1:9, 2:8, 4:6 and 5:5, for M1, M2, M3 and M4, respectively. The ATR-FTIR spectra of CA-39/CA-56 blend membranes for M1 (1:9), M2 (2:8), M3 (4:6) and M4 (5:5) were illustrated in Figure 1.

Based on Figure 1, the wavelengths of the four main bands shown in the graph represented different functional groups found in the CA membranes. The stretching vibration of the ether group (C-O-C) was located at the wavelength of 1034.67 cm^{-1} while the band at 1223.18 cm^{-1} referred to the stretching vibration of the acetyl group (CH_3CO). The 1735.21 cm^{-1} band in the CA membranes corresponded to the carbonyl group (C=O) and the band at 3471.87 cm^{-1} represented the hydroxyl group (O-H).[14,21]

Moreover, Figure 1 illustrated that the intensity of absorbance decreased from M1, M2 to M3 but dramatically increased in M4. When the content of CA-39 increased in the blend membranes, it caused reduction in the absorbance intensity for each main band and demonstrated that fewer functional groups were included in the hydrogen bonding of the blend membranes.[22] In this regard, the presence of polar functional groups influenced the gas permeance as well. Lee et al. stated that the dipole moments of the polar functional groups such as the hydroxyl (O-H) group and the carbonyl (C=O) group in the CA membranes had strong interaction between the CO_2 molecules and the polar functional groups, which affected the absorbance and enhanced the CO_2 permeance.[23] Gassensmith et al. also found that the polar functional groups in the CA membrane bonded with the CO_2 molecules by physisorption manner through dipole interactions.[24] Furthermore, a lower intensity of absorbance indicated that less hydroxyl groups were chemically bonded with acetyl groups and formed polymeric membrane structures with less compactness.[25] However, the increment in the intensity of the absorbance of M4 might be due to the increment in the content of CA-39, which formed strong hydrogen bonding between the water and polymer during membrane formation. This caused disorderly packed polymer chain, which led to a higher intensity of absorbance.[26]

In addition, the SEM was used to investigate the membrane morphology. Thus, the high-resolution cross-section and surface SEM micrographs of CA-39/CA-56 blend membrane for M1 (1 wt% of CA-39), M2 (2 wt% of CA-39), M3 (4 wt% of CA-39) and M4 (5 wt% of CA-39) were presented in Figure 2. The SEM surface images of each membrane, shown in Figures 2(a, c, e and g) show smooth and defect-free surfaces for CA-39/CA-56 blend membranes. The nonporous and dense structure of the CA membrane allowed the build-up of pressure, which is applicable for CO_2/N_2 separation. The smooth and nonporous dense skin layers formed on the upper surface of the membranes were due to the perfect demixing of the CA blend membranes.[27] Besides, the hydrophilic properties

of the CA membranes allowed the formation on the membrane surface with good regularity.[28] It was because of the hydrophilic chains, the hydrophilic CA polymer enriched the membrane surface during the phase separation process through the formation of hydrogen bonding with water molecules.[28,29] Based on Figure 1, the ATR-FTIR analysis showed that the CA membrane had high hydrophilicity due to numerous polar functional groups included in the membranes. Hence, the high hydrophilicity of the CA membranes caused better dispersion in dope solution and formed smooth membrane structures due to the strong hydrogen bonding between the polymer and solvent.[29]

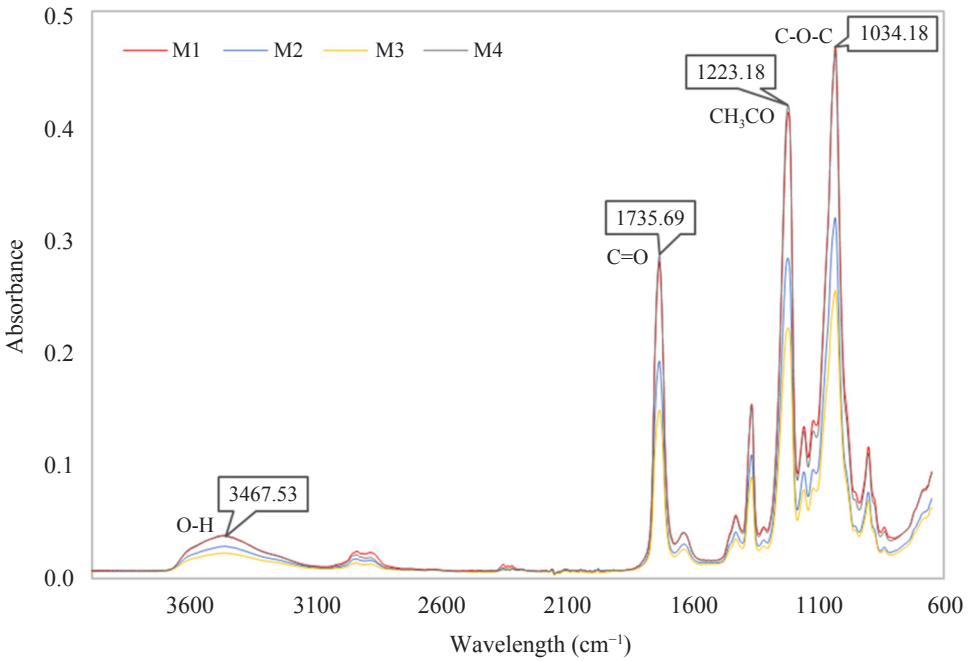

Figure 1: ATR-FTIR spectra for membrane fabricated with polymer ratio of CA with 39% acetyl content to CA with 56% acetyl content at 1:9 (M1), 2:8 (M2), 4:6 (M3) and 5:5 (M4), with constant casting thickness of 250 µm.

Based on Figures 2(b, d, f and h), M1 (6.16 ± 0.07 µm), M2 (5.71 ± 0.07 µm) and M3 (5.47 ± 0.06 µm) had smoother dense skin layer compared to M4 (3.97 ± 0.11 µm). The smooth dense skin layer was formed due to the perfect demixing and precipitation mechanism that tightened the polymer molecular chain.[30] Based on Figure 1, the ATR-FTIR analysis indicated that the strong hydrogen bonding formed between the acetyl group from the CA polymer and carbonyl group from the acetic acid caused stronger interaction between polymer-solvent mixture which led to smoother dense skin layer formation.[13] As observed in Figure 2(h), the M4

demonstrated nonuniformity dense skin layer. It may be due to the increment in CA-39, which was highly hydrophilic than CA-56. The membranes that had high hydrophilic properties with more hydroxyl groups caused irregularities on the dense skin layer due to imperfect demixing mechanism.[26,28,30] The higher hydrophilicity caused water to flow towards the membrane during membrane formation and led to high surface energy and high chances for nonuniform membrane.[31] This was due to the high hydrophilicity of CA-39 leading to strong hydrogen bonding between the water and polymer, thereby, causing water to spread over the membrane during membrane fabrication. The hydrophilic polymer moved towards the membrane surface during the membrane formation process due to its high affinity towards water molecules.[29] Thus, it caused disorderly packed molecules and formed uneven dense skin layer.[26]

In polymeric membranes, the formation of dense skin layer is necessary for CO_2/N_2 separation. The dense skin layer formed by the molecular orientation concentrated on the upper surface of the membrane.[32] As displayed in the SEM images, shown in Figures 2(b, d, f and h), the dense skin layer was observed with reducing thickness from 6.16 ± 0.07 μm (M1) to 3.97 ± 0.11 μm (M4) when the polymer concentration of CA-39 increased from 1 wt% (M1) to 5 wt% (M4). Pinnau and Freeman reported that the higher polymer concentration of polymer with low acetyl content (CA-39) led to thinner dense skin layer formation.[33] When comparing CA-39 with CA-56, the latter contained higher acetyl group content while CA-39 consisted more hydroxyl group which means that the membranes with more CA-39 had higher hydrophilicity.[34] The membrane with higher hydrophilicity, as indicated by the ATR-FTIR analysis, enhanced the polymer and solvent exchange rate when immersing the membrane into distilled water bath. This led to extreme rapid demixing, thus, producing a less dense membrane.[17] Moreover, the increment in polymer concentration of CA-39 increased the hydrophilicity of the polymeric membrane that led to less advanced gelation in polymer/nonsolvent/solvent phase and formed thinner dense skin layer.[17,19] Therefore, the M4 with more CA-39 and less CA-56 resulted in thinner dense skin layer formation.

Based on Figure 2, the final thickness of M1, M2, M3 and M4 were 280.8 ± 1.4 μm, 308.1 ± 1.6 μm, 263.1 ± 0.8 μm and 262.7 ± 1.1 μm, respectively. The decreased membrane thickness led to increase in gas permeation. However, the dense skin layer was the controlling factor for this asymmetric membrane.

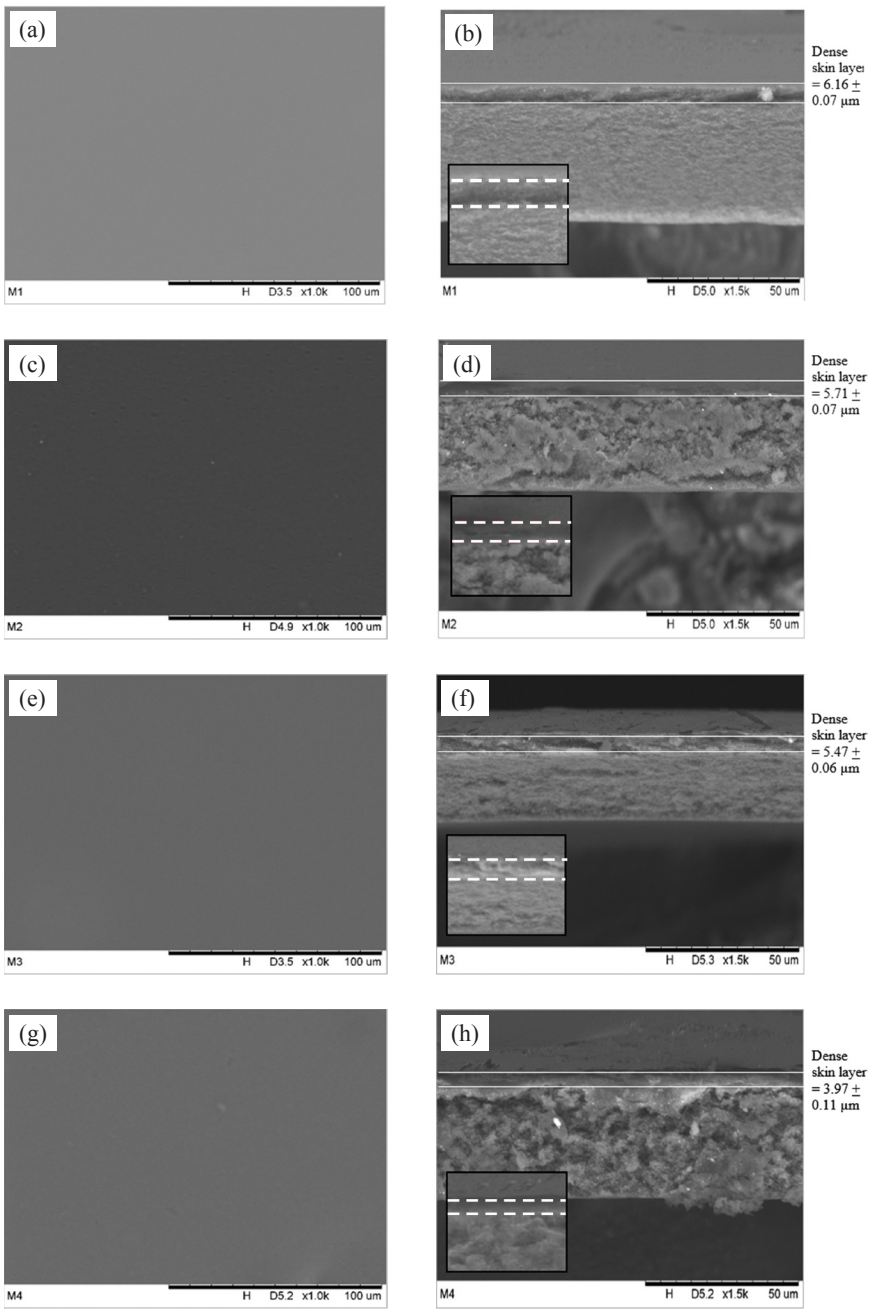

Figure 2: Surface and cross-section SEM images of M1 (a, b), M2 (c, d), M3 (e, f), and M4 (g, h) fabricated with polymer ratio of CA-39 to CA-56 at 1:9, 2:8, 4:6, and 5:5, respectively, with constant casting thickness of 250 µm.

The gas separation performance was determined through the gas permeation test. Figure 3 demonstrates the CO_2 permeance rate of CA-39/CA-56 blend membranes for M1 (1:9), M2 (2:8), M3 (4:6) and M4 (5:5) with polymer concentration of CA-39 at 1 wt%, 2 wt%, 4wt% and 5 wt%, respectively. It showed that the CO_2 permeance improved from 85.64 ± 2.46 GPU (M1) to 328.23 ± 3.09 GPU (M4), when the polymer concentration of CA-39 increased from 1 wt% (M1) to 5 wt% (M4). According to the FTIR analysis and SEM results, indicated in Figure 1 and Figure 2, thinner dense skin layer formation from 6.16 μm to 3.97 μm and lower intensity of absorbance has been observed. This led to higher CO_2 permeance when the polymer content of CA-39 increased. As CA-39 contained less acetyl (CH_3CO) group and more hydroxyl (O-H) group compared to CA-56, more CO_2 was solvated when the polymer content of CA-39 increased, thereby, improving the CO_2 permeance as well.[35] The increment in the hydrophilic CA-39 improved the intramolecular hydrogen bonding between the hydroxyl groups but reduced the intermolecular hydrogen bonding and enhanced the polymer chain rigidity, thus, leading to higher CO_2 permeance.[36] In addition, the increment in the hydrophilic CA-39 formed a stronger interaction between the polar functional groups of the CA polymers and quadrupolar moment of CO_2 which caused improvement in the CO_2 permeance rate.[18,23]

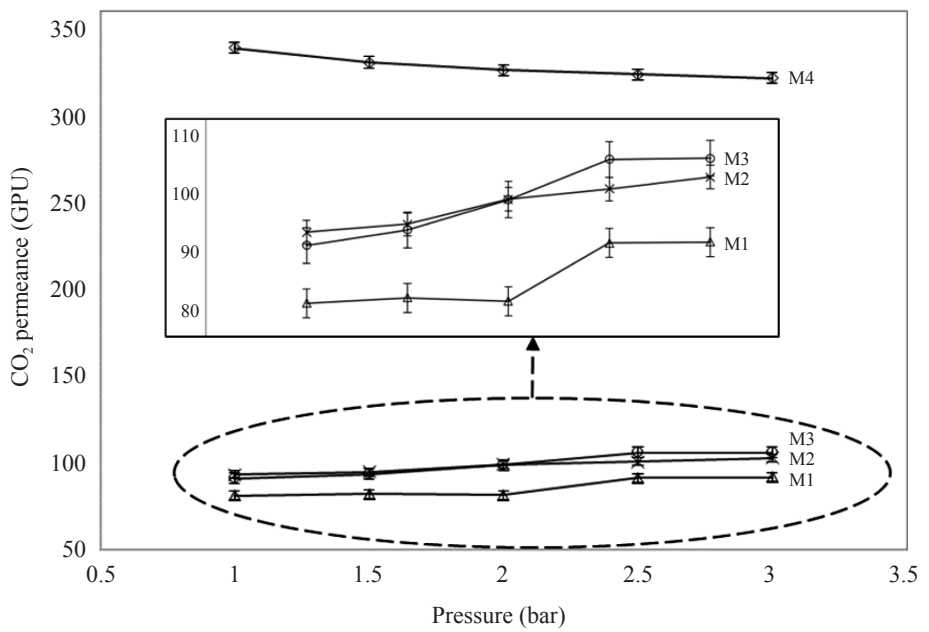

Figure 3: CO_2 permeance rate for M1, M2, M3 and M4, with polymer concentration of CA-39 at 1 wt%, 2 wt%, 4 wt% and 5 wt%, respectively, with constant casting thickness of 250 μm.

Additionally, the CO_2 permeance of M4 (328.23 ± 3.09 GPU) increased dramatically due to the irregular dense skin layer, as demonstrated in Figure 2(h). The nonuniform dense skin layer formed because of the loss of volatile solvent during the membrane fabrication process resulting in reduction in the volatile solvent.[37] The irregular skin layer allowed the CO_2 molecules to pass through the thinner parts of the membrane easily and resulted in high CO_2 permeance.[38]

Figure 4 shows that the N_2 permeation rate increased from about 74.94 ± 1.36 GPU (M1) to 307.05 ± 0.62 GPU (M4) when the polymer content of CA-39 increased from 1 wt% (M1) to 5 wt% (M4). This phenomenon occurred due to the decrease in the dense skin layer from 6.16 ± 0.07 μm, shown in Figure 2(b) to 3.97 ± 0.11 μm, shown in Figure 2(f). Ismail and Yean proved that the membrane with high permeation rate was achieved with thinner dense skin layer.[39] This has been explained by Wijmans and Baker who stated that when the polymer concentration of CA-39 increased, the polymer molecule concentration decreased, thus, causing improvement in gas permeance due to the lesser dense chain packing.[40] Furthermore, the FTIR results showed that when the CA-39 increased, less hydroxyl groups were chemically bonded with the acetyl groups, hence, forming polymeric membrane structure with less compactness that resulted in enhanced N_2 permeance.[25] In addition, the sudden increment in N_2 permeation of M3 (87.12 ± 0.81 GPU) to M4 (307.05 ± 0.62 GPU) may be due to the irregular dense skin layer thickness of M4. The formation of irregular dense skin layer caused faulty polymer chain distribution and allowed the N_2 particles to permeate through the membrane easily. This may due to the insufficient dispersion of the polymer in dope solution and imperfect polymer chain packing.[29,39]

Based on Figure 5, the CO_2/N_2 selectivity for CA-39/CA-56 blend membrane decreased when the polymer concentration of CA-39 increased from 1 wt% (M1) to 5 wt% (M4). The CO_2/N_2 selectivity of M1, M2 and M3 were 1.1428 ± 0.02, 1.1406 ± 0.034 and 1.139 ± 0.037, respectively. Madaeni et al. explained that the increment in gas permeance rate lead to lower selectivity for the polymeric membrane.[12] Furthermore, the dense skin layer thickness reduced from 6.16 ± 0.07 μm, shown in Figure 2(b), to 3.97 ± 0.11 μm, shown in Figure 2(f). When the dense skin layer thickness decreased, the layers formed in membrane formation were reduced in each membrane and led to lower resistance against the passing gas that caused lower membrane selectivity.[13,41]

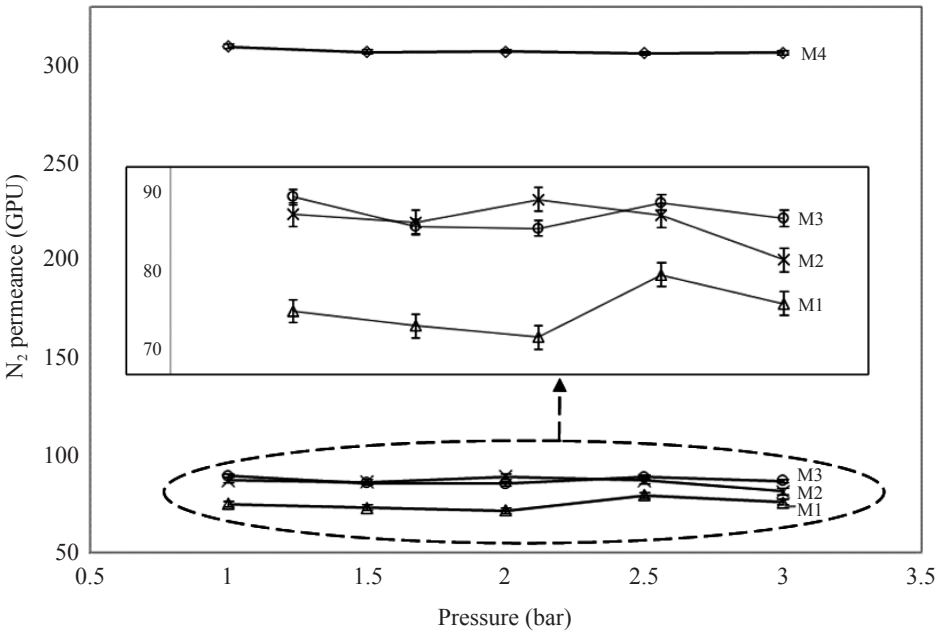

Figure 4: N_2 permeance rate for M1, M2, M3 and M4, with polymer concentration of CA-39 at 1 wt%, 2 wt%, 4 wt% and 5 wt %, respectively, with constant casting thickness of 250 μm.

The results also illustrated that M4 had the lowest selectivity, which was 1.069 ± 0.008. This was due to the irregular dense skin layer formation that enabled both the CO_2 and N_2 gas particles to permeate through the membrane easily. Ahmad et al. reported that the selectivity of membrane strongly depended on the integrity of the dense skin layer.[18] Therefore, to obtain a high selectivity membrane, the dense skin layer formed must be uniform and dense.

Besides, the reduction of CO_2/N_2 selectivity occurred due to lower molecular concentration when more CA-39 was used. It caused less dense polymer chain packing and low complexity on side group, with more hydroxyl groups and less acetyl groups, leading to poor polymer chain distribution and low selectivity.[42] Due to the increment in gap size between polymer chain, the selectivity for the membrane decreased because of the low resistance to gas permeance.[41]

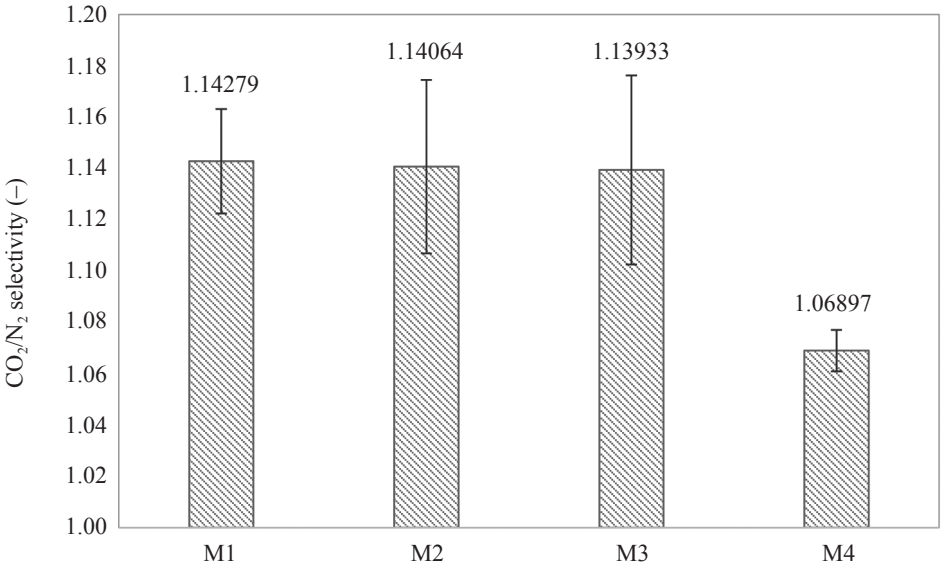

Figure 5: Average CO_2/N_2 selectivity for membrane fabricated with polymer ratio of CA-39 to CA-56 at 1:9 (M1), 2:8 (M2), 4:6 (M3) and 5:5 (M4), with constant casting thickness of 250 μm.

In summary, Figure 6 was exhibited to summarise the average CO_2 permeance, N_2 permeance and CO_2/N_2 selectivity of every membrane. It proved that the CO_2 had higher permeation rate than N_2 for each membrane. This result was presented because the high condensable CO_2 had better interaction with the polymeric chain and functional groups of the CA membrane compared with N_2, due to its quadrupolar moment.[18] Hence, this resulted in a higher CO_2 permeance than N_2 permeance. Based on the results, the percentage of decrement in CO_2/N_2 selectivity among M1 (1 wt% of CA-39), M2 (2 wt% of CA-39) and M3 (4 wt% of CA-39) were negligible. However, the CO_2/N_2 selectivity exhibited reduction between M3 (4 wt% of CA-39) and M4 (5 wt% of CA-39) from 1.139 ± 0.037 to 1.069 ± 0.008, respectively. Therefore, although M4 had extremely high CO_2 permeance and N_2 permeance, it was still eliminated. Thus, M3 was selected as the best membrane due to its relatively high CO_2 permeance, N_2 permeance and CO_2/N_2 selectivity (99.26 ± 3.08 GPU, 87.12 ± 0.81 GPU and 1.139 ± 0.037, respectively).

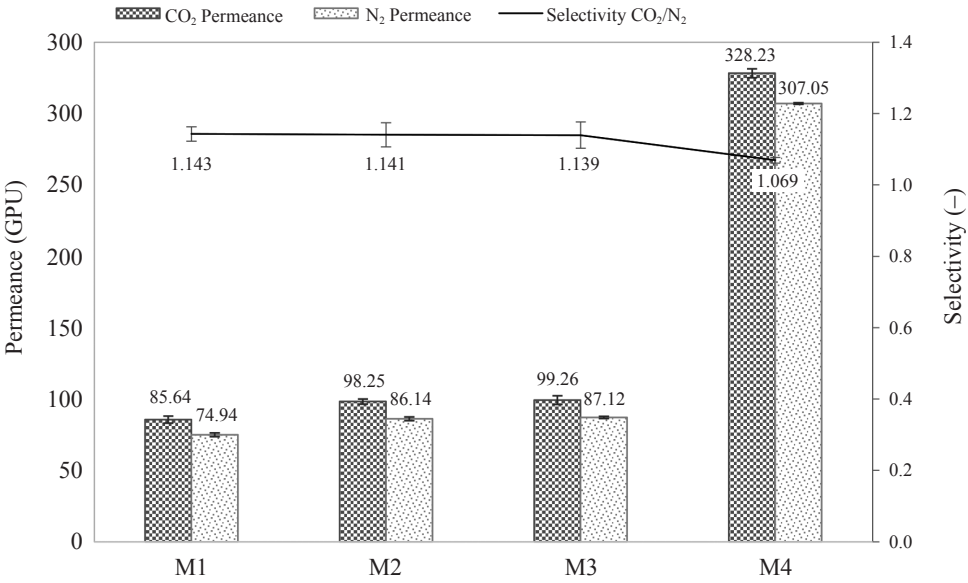

Figure 6: Average CO_2 permeance, N_2 permeance and CO_2/N_2 selectivity for M1, M2, M3 and M4, with polymer ratio of CA-39 to CA-56 at 1:9, 2:8, 4:6 and 5:5, respectively, with constant casting thickness of 250 μm.

Ultimately, the results investigated in this study were compared with other research works of Farrukh et al. and Moghadasi et al. working on CA membrane fabrication, illustrated in Table 2.[17,43] Farrukh et al. prepared a pure CA membrane by using the CA polymer with acetyl concentration of 39.8% and studied the CO_2/N_2 gas separation performance.[17] Table 2 demonstrated that higher CO_2 permeance and N_2 permeance were found for the optimal blend CA membrane (M3) in the present work, while comparing with Farrukh et al.[17] However, the CO_2/N_2 selectivity was lower than the available membrane. This was due to the extremely strong interaction formed between the hydroxyl groups and the acetyl groups which caused high compactness membrane that led to low gas permeance and high membrane selectivity.[22,25] Furthermore, the presence of CA-56 with more acetyl groups in the CA polymer matrix caused movement in the polymeric chains, which improved the gas permeability.[1,20,35] This study was at preliminary level. Therefore, more researches are required to understand the blending chemistry of CA polymers in order to improve the gas separation performance effectively.

Table 2: Comparison of gas separation performance between present work and other research studies.

References	CA membrane	CO_2 permeance	N_2 permeance	CO_2/N_2 selectivity
Present work	M3	2.48*	2.18*	1.139
Farrukh et al.[17]	Pure CA with acetyl content 38.9%	1.062#	0.743#	1.429
Moghadasi et al.[43]	CA	1.08#	0.44#	2.45

*Notes: * GPU, # barrer*

4. CONCLUSION

In this work, new membranes were successfully fabricated by blending the CA-39 and CA-56. The gas separation performance for the CA-39/CA-56 blend membranes were proven to be affected by the polymer concentration. The optimal CA-39/CA-56 blend membrane, M3, with the polymer ratio (CA-39:CA-56) at 4:6, was determined. The ATR-FTIR spectrum successfully indicated that the CA-39/CA-56 blend membrane consisted of polar functional groups that favoured the CO_2 permeance. The SEM results indicated that M3 formed a membrane that had relatively thin dense skin layer with smooth surface and uniform structure which demonstrated integrity of membrane structure and allowed the application of solution-diffusion mechanism. Besides, the M3 had the best CO_2 permeance, N_2 permeance and CO_2/N_2 selectivity which were 99.26 ± 3.08, 87.12 ± 0.81 and 1.139 ± 0.037, respectively. Therefore, M3 demonstrated higher CO_2 and N_2 permeation rates but relatively lower selectivity for CO_2/N_2 separation. In the future, it is expected that the mixed matrix membrane will improve the gas separation performance by combining the advantages of both polymeric and inorganic components while hollow fibre membrane performs high compactness and self-supported membrane structure.

5. ACKNOWLEDGEMENTS

The authors wish to express gratitude to the Ministry of Higher Education Malaysia (MOHE) for financial support through the Fundamental Research Grant Scheme (FRGS) (no. FRGS/1/2015/TK02/CURTIN/03/1) and Cost Centre 001048. Other financial backers that the authors would also like to thank are Long-term Research Grant (LRGS), Universiti Sains Malaysia (no. 304/PJKIMIA/6050296/U124), and Curtin Cost Centre 001047.

6. REFERENCES

1. Powell, C. E. & Qiao, G. G. (2006). Polymeric CO_2/N_2 gas separation membranes for the capture of carbon dioxide from power plant flue gases. *J. Membr. Sci.*, 279(1), 1–49. https://doi.org/10.1016/j.memsci.2005.12.062
2. Siagian, U. W. R. et al. (2019). Membrane-based carbon capture technologies: Membrane gas separation vs. membrane contactor. *J. Nat. Gas Sci. Eng.*, 67, 172–195. https://doi.org/10.1016/j.jngse.2019.04.008
3. Sun, J. et al. (2017). CO_2 separation membranes with high permeability and CO_2/N_2 selectivity prepared by electrostatic self-assembly of polyethylenimine on reverse osmosis membranes. *RSC Adv.*, 7(24), 14678–14687. https://doi.org/10.1039/C7RA00094D
4. Liang, C. Z. et al. (2019). A review of polymeric composite membranes for gas separation and energy production. *Prog. Polym. Sci.*, 97, 101141. https://doi.org/10.1016/j.progpolymsci.2019.06.001
5. He, J. et al. (2017). A literature research on the performance evaluation of hydrate-based CO_2 capture and separation process. *Energy Procedia*, 105, 4090–4097. https://doi.org/10.1016/j.egypro.2017.03.867
6. Mubashir, M. et al. (2018). Efficient CO_2/N_2 and CO_2/CH_4 separation using NH_2-MIL-53(Al)/cellulose acetate (CA) mixed matrix membranes. *Sep. Purif. Technol.*, 199, 140–151. https://doi.org/10.1016/j.seppur.2018.01.038
7. Feron, P. H. M. et al. (1992). Membrane technology in carbon dioxide removal. *Energy Convers. Manag.*, 33(5), 421–428. https://doi.org/10.1016/0196-8904(92)90039-Y
8. Houde, A. Y. & Stern, S. A. (1997). Solubility and diffusivity of light gases in ethyl cellulose at elevated pressures effects of ethoxy content. *J. Membr. Sci.*, 127(2), 171–183. https://doi.org/10.1016/S0376-7388(96)00266-9
9. Thakur, V. K. & Voicu, S. I. (2016). Recent advances in cellulose and chitosan based membranes for water purification: A concise review. *Carbohydr. Polym.*, 146, 148–165. https://doi.org/10.1016/j.carbpol.2016.03.030
10. Aroon, M. A. et al. (2010). Morphology and permeation properties of polysulfone membranes for gas separation: Effects of non-solvent additives and co-solvent. *Sep. Purif. Technol.*, 72(2), 194–202. https://doi.org/10.1016/j.seppur.2010.02.009
11. Hacarlioglu, P. et al. (2003). Effect of preparation parameters on performance of dense homogeneous polycarbonate gas separation membranes. *J. Appl. Polym. Sci.*, 90(3), 776–785. https://doi.org/10.1002/app.12505
12. Madaeni, S. S., Enayati, E. & Vatanpour, V. (2011). The influence of membrane formation parameters on structural morphology and performance of PES/PDMS composite membrane for gas separation. *J. Appl. Polym. Sci.*, 122(2), 827–839. https://doi.org/10.1002/app.34066
13. Jawad, Z. A. et al. (2015). Incorporation of inorganic carbon nanotubes fillers into the CA polymeric matrix for improvement in CO_2/N_2 separation. *Curr. Nanosci.*, 11, 69–79. https://doi.org/10.2174/1573413710666140922224633

14. Jawad, Z. A. et al. (2016). The role of solvent mixture, acetic acid and water in the formation of CA membrane for CO_2/N_2 separation. *Procedia Eng.*, 148, 327–332. https://doi.org/10.1016/j.proeng.2016.06.446
15. Ahmad, A. L. et al. (2014). A cellulose acetate/multi-walled carbon nanotube mixed matrix membrane for CO_2/N_2 separation. *J. Membr. Sci.*, 451, 55–66. https://doi.org/10.1016/j.memsci.2013.09.043
16. Li, D., Yao, J. & Wang, H. (2013). CO_2 selective separation membranes. In Zhou, Y. (Ed.), *Eco- and renewable energy materials*. Berlin: Springer Berlin Heidelberg, 259–309.
17. Farrukh, S. et al. (2014). Blending of TiO_2 nanoparticles with cellulose acetate polymer: To study the effect on morphology and gas permeation of blended membranes. *Asia Pac. J. Chem. Eng.*, 9(4), 543–551. https://doi.org/10.1002/apj.1783
18. Ahmad, A. L. et al. (2017). Thickness effect on the morphology and permeability of CO_2/N_2 gases in asymmetric polyetherimide membrane. *J. Phys. Sci.*, 28(Supp. 1), 201–213. https://doi.org/10.21315/jps2017.28.s1.13
19. Nguyen, T. P. N. et al. (2013). Preparation of cellulose triacetate/cellulose acetate (CTA/CA)-based membranes for forward osmosis. *J. Membr. Sci.*, 433, 49–59. https://doi.org/10.1016/j.memsci.2013.01.027
20. Farrukh, S. et al. (2014). Preparation, characterization, and applicability of novel calix[4]arene-based cellulose acetate membranes in gas permeation. *J. Appl. Polym. Sci.*, 131(6). https://doi.org/10.1002/app.39985
21. Sanaeepur, H. et al. (2019). Pebax-modified cellulose acetate membrane for CO_2/N_2 separation. *J. Membr. Sci.*, 5(1), 25–32. https://doi.org/10.22079/jmsr.2018.85813.1190
22. Mendes, G. et al. (2018). Structure of water in hybrid cellulose acetate-silica ultrafiltration membranes and permeation properties. *Carbohydr. Polym.*, 189, 342–351. https://doi.org/10.1016/j.carbpol.2018.02.030
23. Lee, H. M. et al. (2015). Interactions of CO_2 with various functional molecules. *Phys. Chem. Chem. Phys.*, 17(16), 10925–10933. https://doi.org/10.1039/C5CP00673B
24. Gassensmith, J. J. et al. (2011). Strong and reversible binding of carbon dioxide in a green metal-organic framework. *J. Am. Chem. Soc.*, 133(39), 15312–15315. https://doi.org/10.1021/ja206525x
25. Puleo, A. C. et al. (1989). The effect of degree of acetylation on gas sorption and transport behavior in cellulose acetate. *J. Membr. Sci.*, 47(3), 301–332. https://doi.org/10.1016/S0376-7388(00)83083-5
26. Li, G. et al. (2013). Cellulose triacetate forward osmosis membranes: Preparation and characterization. *Desalin. Water. Treat.*, 13–15(51), 2656–2665. https://doi.org/10.1080/19443994.2012.749246
27. Sridhar, S., S. Bee, & S. Bhargava, (2014), Membrane-based gas separation: Principle, applications and future potential. *Chem. Eng. Dig.*, 1–25.
28. Hossein Razzaghi, M. et al. (2014). Morphological and separation performance study of PVDF/CA blend membranes. *J. Membr. Sci.*, 470, 547–557. https://doi.org/10.1016/j.memsci.2014.07.026

29. Kumar, R. & Ismail, A. F. (2015). Fouling control on microfiltration/ultrafiltration membranes: Effects of morphology, hydrophilicity, and charge. *J. Appl. Polym. Sci.*, 132(21). https://doi.org/10.1002/app.42042
30. Abd Rahman, S. et al. (2004). Formation of cellulose acetate membrane for gas separation from binary dope system: Effect of shear rate. Paper presented at the Proceedings of Regional Symposium on Membrane Science and Technology, 21–25.
31. Kamal, H. et al. (2014). Characterization and some properties of cellulose acetate-co-polyethylene oxide blends prepared by the use of gamma irradiation. *J. Radiat. Res. Appl. Sci.*, 7(2), 146–153. https://doi.org/10.1016/j.jrras.2014.01.003
32. Mohamed, F. et al. (2016). Effect of coagulant bath on the gas permeation properties of cellulose acetate asymmetric membrane. *IOP Conf. Ser. Earth Environ. Sci.*, 36(1), 012009.
33. Pinnau, I. & Freeman, B. D. (2000). Membrane formation and modification: Overview. *ACS Symp. Ser.*, 744, 1–12. https://doi.org/10.1021/bk-2000-0744.ch001
34. Romero, R. B. et al. (2009). The effect of the solvent on the morphology of cellulose acetate/montmorillonite nanocomposites. *Polym. J.*, 50(1), 161–170. https://doi.org/10.1016/j.polymer.2008.10.059
35. Li, J. et al. (1998). Effect of polyethyleneglycol (PEG) on gas permeabilities and permselectivities in its cellulose acetate (CA) blend membranes. *J. Membr. Sci.*, 138(2), 143–152. https://doi.org/10.1016/S0376-7388(97)00212-3
36. Mubashir, M. et al. (2018). Enhanced gases separation of cellulose acetate membrane using N-methyl-1-2 pyrrolidone as fabrication solvent. *Int. J. Autom. Mech. Eng.*, 15(1), 4978–4986.
37. Uragami, T. (2017). *Science and technology of separation membranes.* Delhi: John Wiley & Sons.
38. Houde, A. Y. et al. (1996). Permeability of dense (homogeneous) cellulose acetate membranes to methane, carbon dioxide, and their mixtures at elevated pressures. *J. Appl. Polym. Sci.*, 62(13), 2181–2192. https://doi.org/10.1002/(SICI)1097-4628(19961226)62:13<2181::AID-APP1>3.0.CO;2-F
39. Ismail, A. F. & Yean, L. P. (2003). Review on the development of defect-free and ultrathin-skinned asymmetric membranes for gas separation through manipulation of phase inversion and rheological factors. *J. Appl. Polym. Sci.*, 88(2), 442–451. https://doi.org/10.1002/app.11744
40. Wijmans, J. G. & Baker, R. W. (1995), The solution-diffusion model: A review. *J. Membr. Sci.*, 107(1), 1–21. https://doi.org/10.1016/0376-7388(95)00102-I
41. Paul, D. R. & Yampolskii, Y. P. (2018). *Polymeric gas separation membrane*. New York: Taylor & Francis.
42. Ismail, A. F., Khulbe, K. & Matsuura, T. (2015). *Gas separation membranes: Polymeric and inorganic*. Bern: Springer International Publishing.
43. Moghadasi, A. R. et al. (2014). Fabrication and modification of cellulose acetate based mixed matrix membrane: Gas separation and physical properties. *J. Ind. Eng. Chem.*, 20(3), 1050–1060. https://doi.org/10.1016/j.jiec.2013.06.042